

See discussions, stats, and author profiles for this publication at: <https://www.researchgate.net/publication/373256379>

# Science of Climate Change About Historical CO<sub>2</sub>-Data since 1826: Explanation of the Peak around 1940

Article · August 2023

DOI: 10.53234/scc202304/21

---

CITATIONS

0

---

READS

162

1 author:



**Hermann Harde**

Helmut Schmidt University Hamburg

119 PUBLICATIONS 1,322 CITATIONS

SEE PROFILE



*Klimarealistene*  
P.O. Box 33,  
3901 Porsgrunn  
Norway  
ISSN: 2703-9072

Correspondence:  
harde@hsu-hh.de

Vol. 3.2 (2023)

pp. 211-218

## About Historical CO<sub>2</sub>-Data since 1826:

### Explanation of the Peak around 1940

*Hermann Harde*

*Helmut-Schmidt-University, Hamburg, Germany*

#### Abstract

Recently a compilation of almost 100.000 historical data about chemical CO<sub>2</sub> concentration measurements between 1826 and 1960 has been published as post mortem memorial edition of the late Ernst-Georg Beck. This compilation can give important insight in understanding natural CO<sub>2</sub> emission processes, but it has been criticized, in particular a documented significant increase of the atmospheric CO<sub>2</sub> concentration around 1940. In this contribution we do not respond to any criticism of more or less suitable places for sampling or the interpretation of respective data, but concentrate on the CO<sub>2</sub> data around 1940 and the variations over the last century. We show that the observed concentration changes not only correlate with observed temperatures, but can also quantitatively be explained, mainly in terms of the temperature dependent soil respiration.

**Keywords:** CO<sub>2</sub> mixing ratio; direct chemical measurement; natural CO<sub>2</sub> emission, soil respiration; oceanic CO<sub>2</sub> emissions

Submitted 2023-05-15, Accepted 2023-06-08,

<https://doi.org/10.53234/scc202304/21>

#### 1. Introduction

Our knowledge about paleoclimatic variations of CO<sub>2</sub> concentration in the atmosphere is exclusively based on proxy data. But such indirect measurements from ice cores, tree rings, stalactites or stomata suffer from higher time resolution, sensitivity and accurate calibration of the data. Therefore, before the implementation of infrared spectroscopy analyses in 1958 for atmospheric CO<sub>2</sub> concentration measurements, with the development of chemical techniques in the early 19<sup>th</sup> century it was a great progress to have a direct method available for the detection of the CO<sub>2</sub> level. But unfortunately, these data were not systematically prepared or compiled, and instead, paleoclimatic research was only concentrating on the less accurate proxy data.

Luckily, with a more than 12 years delayed publication of a monumental data set of the late Ernst-Georg Beck (Beck 2022), new insight into variations of the CO<sub>2</sub> concentration over the 19<sup>th</sup> century and the first half of the 20<sup>th</sup> century can be derived. Special thanks to H. Yndestad (2022), and J.-E Solheim as Chief-Editor of this journal for making available this publication. Beck found more than 200,000 single samples of air analyzed with chemical methods, showing daily, yearly and seasonal variations, which were published in 979 technical papers. He selected almost 100,000 samples associated with documented meteorological conditions between CO<sub>2</sub>, wind speed, precipitation, day time and year. This gave the opportunity to determine atmospheric CO<sub>2</sub> concentrations with an accuracy, at least an order of magnitude better than from proxy data, and he concluded that there are repeated fluctuations in concert with the surface temperature variations of the sea.

In an actual article (Engelbeen 2023) the historical data were criticized that many places were completely unsuitable for “background” CO<sub>2</sub> level measurements and that Beck made several mistakes in the interpretation of the available data. Particularly, the huge CO<sub>2</sub> levels around 1940

would be physically impossible and contradict several other proxies as measured in high resolution ice cores.

While it is out of the scope of this contribution to comment on the unsuitability of places, the number of measurements at higher wind speed (to have a sufficient convergence of data) or on any mistakes in the interpretation, we look closer to the measured CO<sub>2</sub> levels around 1940.

In Section 2 we briefly review the temperature sensitivity of oceanic and land emissions with their expected contributions to the atmospheric CO<sub>2</sub> mixing ratio (for further details see: Salby & Harde 2022). Simulations with a land-air temperature series (Soon et al. 2015) alone or in combination with sea surface data (HadSST4, Kennedy et al. 2019) can well reproduce an increased concentration over the 30s to 50s and the further evolution over the last century. Particularly soil respiration in the tropics and mid-latitudes can be identified as the main natural source. Different to a pure correlation of time series, our studies give a clear physical explanation with a quantitative reproduction of the observed data.

## 2. Relationship of Temperature and Atmospheric CO<sub>2</sub>-Concentration

Beck's historical data compilation consists of 97,404 samples of atmospheric CO<sub>2</sub> mixing ratios, which were derived from 901 stations and cover a period from 1826 to 2008. The data show a pronounced maximum between 1939 and 1943 with a concentration up to 383 ppm, this in contrast to the monotonically rising CO<sub>2</sub>-levels reconstructed from ice cores. Alone the data around this maximum from 1930 to 1950 represent about 60,000 samples and are based on the work of more than 25 different authors and locations.

The time resolution and accuracy of this data series is much better compared to reconstructions from ice core data and even from stomata. Therefore, for serious climate studies it is of fundamental importance and interest to better understand possible forcings that can explain strongly varying CO<sub>2</sub> levels, particularly over periods, for which more reliable meteorological and astrophysical data are available than this is the case for paleontological times. At the same time, stronger anthropogenic impacts over this period can be largely excluded. So, it sounds pretty inconvincible, when Engelbeen (2023) comments that "*the possibility of huge CO<sub>2</sub> levels around 1940 is physically impossible and contradicted by several other proxy's and contradicted by CO<sub>2</sub> levels as measured in high resolution ice cores.*"

Beck already found a high correlation of the CO<sub>2</sub> level data to the global Sea Surface Temperature (SST) series of the Royal Netherlands Meteorological Institute (Kaplan, KNMI). Supported by different observations of CO<sub>2</sub> enriched air at the coast (North Sea, Barents Sea, Northern Atlantic) he suggested that warmer ocean currents over the Northern Atlantic are the sources of the enhanced CO<sub>2</sub>-levels.

Different studies confirm outgazing of warmer oceans, particularly the tropical oceans, as sources of CO<sub>2</sub>. But they also show that the oceanic CO<sub>2</sub> emission  $E_O$  as flux  $F_O$ , weighted by its fractional surface area  $S_O$  as

$$E_O = S_O F_O \cong S_O B(v) \Delta r \quad (1a)$$

depends primarily upon wind speed  $v$  and the atmosphere-ocean contrast  $\Delta r = r_O - r_A$  (Wanninkhof 2014) with  $r_O$  as the CO<sub>2</sub> mixing ratio of the ocean and  $r_A$  as mixing ratio of the atmosphere. The temperature sensitivity to oceanic emission

$$Q_O = \frac{1}{E_O} \frac{dE_O}{dT_O} \cong 3 \text{ \%}/^\circ\text{C} \quad (1b)$$

with  $T_O$  as the mean ocean temperature is relatively small (Salby & Harde 2022, eq. (20)).

Different to the oceans, CO<sub>2</sub> emission  $E_L$  over land with the flux  $F_L$  and fractional area weighting  $S_L$  follows from soil respiration  $R$

$$E_L = S_L F_L \cong S_L R(T_L, m_L), \quad (2a)$$

which depends upon soil temperature  $T_L$  and moisture  $m_L$  (see: Salby & Harde 2022, eqs (6.1) and (6.2)). Soil respiration  $R$  derives from microbial activity and upward diffusion of the produced CO<sub>2</sub> (cf. Maier et al. 2020). It is noteworthy that the partial pressure of CO<sub>2</sub> in soil and its mixing ratio  $r_L$  with 500 - 20,000 ppmv vastly exceeds the atmospheric mixing ratio  $r_A$ .

For a uniform perturbation of surface conditions, the enormous partial pressures of CO<sub>2</sub>, found just a few tens of cm beneath the surface, makes emission from land determinative in re-establishing equilibrium between the atmosphere and the Earth's surface.

Although  $R$  is influenced by soil moisture, it is controlled chiefly by surface temperature (Wood et al. 2013; Zhou et al. 2013), which is determined by air temperature, i.e.,  $F_L \cong R(T_L)$ . The temperature sensitivity of soil respiration,

$$Q_L = \frac{1}{R} \frac{dR}{dT_L} = \frac{1}{E_L} \frac{dE_L}{dT_L} \quad (2b)$$

is observed in the range 10%/°C - 25%/°C at temperate and polar latitudes (Raich & Schlesinger 1992; Lloyd and Taylor 1994). In tropical forest, however, copious precipitation and sunlight magnify active biomass, which supports soil respiration. There, the observed sensitivity to temperature is greatest (ibid; Brechet et al. 2018), 30%/°C and higher (Wood et al. 2013; Nottingham et al. 2018). This is roughly about one order of magnitude larger than the oceanic sensitivity  $Q_O$  with  $\approx 3\%/^{\circ}\text{C}$ . Therefore, despite the smaller land surface area, soil respiration can well be considered as comparable or even as the dominating temperature dependent source of CO<sub>2</sub>.

### 2.1 Relative Contributions of Ocean and Land

The fractional perturbation of atmospheric CO<sub>2</sub>,  $\delta r_A/r_A$  equals the fractional perturbation of total emission,  $\delta E_T/E_T$ , independently of effective absorption (see: Salby & Harde 2022, eq. (26)):

$$\frac{\delta r_A}{r_A} = \frac{\delta E_O + \delta E_L}{E_O + E_L} \quad (3)$$

According to marine observations of  $\Delta r$  (Takahashi 1997; Feely et al. 2001) and satellite observations of CO<sub>2</sub>, particularly over tropical land (Palmer et al. 2019), emission from tropical ocean and land surface lie in the range

$$0.63E_O < E_L < 4.57E_O. \quad (4a)$$

With (3) it follows (see: Salby & Harde 2022, Appendix A) that the fractional increase of atmospheric CO<sub>2</sub> must lie in the range:

$$0.39 \cdot Q_L \cdot \delta T_L < \frac{\delta r_A}{r_A} < 0.02 + 0.82 \cdot Q_L \cdot \delta T_L, \quad (4b)$$

with a medium value  $m \approx 0.6$  for the thermally-induced increase of atmospheric CO<sub>2</sub>, collectively from ocean and land

$$\frac{\delta r_A}{r_A} \approx m \cdot Q_L \cdot \delta T_L. \quad (4c)$$

Integration of (4c) gives the atmospheric mixing ratio as a function of the land air temperature:

$$r_A(\delta T_L) \approx r_A(0) \cdot e^{m \cdot Q_L \cdot \delta T_L}, \quad (5a)$$

with  $r_A(0)$  as mixing ratio at preindustrial times.

Including also anthropogenic emissions  $\delta E_A$  over the Industrial Era, (3) expands by this additional term  $\delta E_A$  in the numerator, while the total emission  $E_T$  in the denominator stays unchanged. Thus, (4c) expands by the additional term  $\delta E_A/E_T$ , which at equilibrium and due to the conservation law

with  $r_A = E_T \tau_{eff}$  and  $\tau_{eff}$  as the effective absorption time converts (5a) to:

$$r_A(\delta T_L) \approx r_A(0) \cdot e^{m \cdot Q_L \cdot \delta T_L} + \delta E_A \cdot \tau_{eff}. \quad (5b)$$

In Fig. 1 is plotted the rural-only land air temperature anomaly of the Northern Hemisphere (Green Squares) over the period 1870 to 2014 (see: Soon et al. 2015). The number of stations used for each year over the relevant interval 1930 to 1950 is typically 300. The data represent an average over 3 years. This series was chosen, as it represents most directly any variations of the land emissions  $E_L$  with temperature.

The calculated CO<sub>2</sub> mixing ratio as a function of the rural land air temperature anomaly  $\delta T_L$  and the anthropogenic emissions  $\delta E_A$  is plotted as Red Diamonds for  $m = 0.6$  and a temperature sensitivity  $Q_L = 30\%/^{\circ}\text{C}$ , as expected for soil respiration in the tropics to mid-latitudes. For the fossil fuel emissions and land use changes we refer to the CDIAC data (2017), and for the effective absorption or residence time we use  $\tau_{eff} \approx 3.5$  yrs in agreement with IPCC (AR5 2013, Fig. 6.1; AR6 2021, Fig. 5.12; Harde 2017; Harde & Salby 2021). Comparison with the historical CO<sub>2</sub> data (Dark Dots) shows that the calculation confirms an increased emission and mixing ratio over the 30s to 50s, only with a broader and reduced maximum than the CO<sub>2</sub> observations. Also the observed increasing concentration over the Mauna Loa Era (Light Blue Dots) can well be reproduced by the thermally induced emissions, while the anthropogenic emissions over this period will not contribute more than  $\delta r_{A,ant} = \delta E_{A,max} \cdot \tau_{eff} \approx 12$  ppmv (assuming equilibrium).

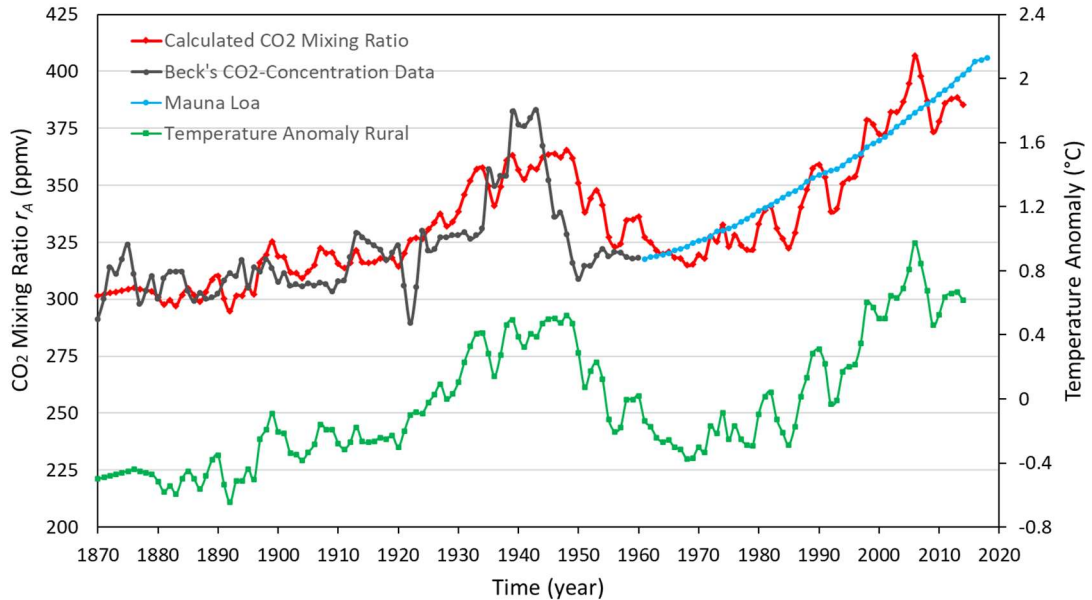


Fig. 1: Comparison of Beck's historical CO<sub>2</sub> concentration (Dark Dots) with calculation (Red Diamonds) for  $m = 0.6$  and  $Q_L = 30\%/^{\circ}\text{C}$ , based on Northern Hemisphere rural land air temperature data (Green Squares, Soon et al. 2015) over a period of 145 yrs. Additionally this is compared with the Mauna Loa observations (Light Blue Dots, CDIAC 2017).

## 2.2 Alternative Consideration of Oceanic and Land Emission

A slightly different derivative for the contributions of ocean and land starts again from (3), including the anthropogenic emissions  $\delta E_A$ . Integration of (1b) and (2b) gives:

$$\delta E_k = E_k (e^{Q_k \delta T_k} - 1), \quad k = O, L. \quad (6a)$$

With a relative weighting  $w = E_L/E_O$  and  $E_T = E_O + E_L$ , together with (3), including human emissions, the fractional perturbation  $\delta r_A/r_A$  then can be written as:

$$\frac{\delta r_A}{r_A} = \frac{1}{E_T} \left\{ \frac{E_T}{1+w} (e^{Q_O \delta T_O} - 1) + \frac{w \cdot E_T}{1+w} (e^{Q_L \delta T_L} - 1) + \delta E_A \right\}, \quad (6b)$$

and together with  $r_A = E_T \tau_{eff}$ , the atmospheric mixing ratio as a function of the temperature anomalies  $\delta T_L$  and  $\delta T_O$  and also the anthropogenic emissions  $\delta E_A$  then becomes:

$$r_A(\delta T_L, \delta T_O) \approx r_A(0) \frac{e^{Q_O \cdot \delta T_O} + w e^{Q_L \cdot \delta T_L}}{1 + w} + \delta E_A \cdot \tau_{eff}. \quad (6c)$$

Fig. 2 displays the respective calculation with this modified derivation of combined emissions for a weighting  $w = 2$ , i.e., with land emissions  $E_L$  twice the oceanic emissions  $E_O$  (Red Diamonds). The respiration was again calculated for  $Q_L = 30\%/^{\circ}\text{C}$  and using the Northern Hemisphere rural-only temperature anomaly (Green Squares, Soon et al. 2015). The oceanic emissions were calculated with a temperature sensitivity  $Q_O = 3\%/^{\circ}\text{C}$  and applying the sea surface temperature anomaly HadSST4 of the Met Office Hadley Centre (Blue Triangles, Kennedy et al. 2019). Anthropogenic emissions are the same as in Subsection 2.1.

This simulation is quite similar to Fig. 1, as it is clearly dominated by the strongly temperature dependent respiration, while the oceanic emissions, mainly controlled by the atmosphere-ocean contrast and wind speed (see eq. (1)), only supply an almost constant background of one third to the total emissions. In comparison to the historical observations (Dark Dots) the maximum around 1940 can well be reproduced with an assumed weighting of two, only the CO<sub>2</sub> measurements indicate a faster decay over the 40s, before the mixing ratio is again increasing with temperature. A smaller weighting  $w$  slightly reduces the maximum around the 40s and the consecutive increase.

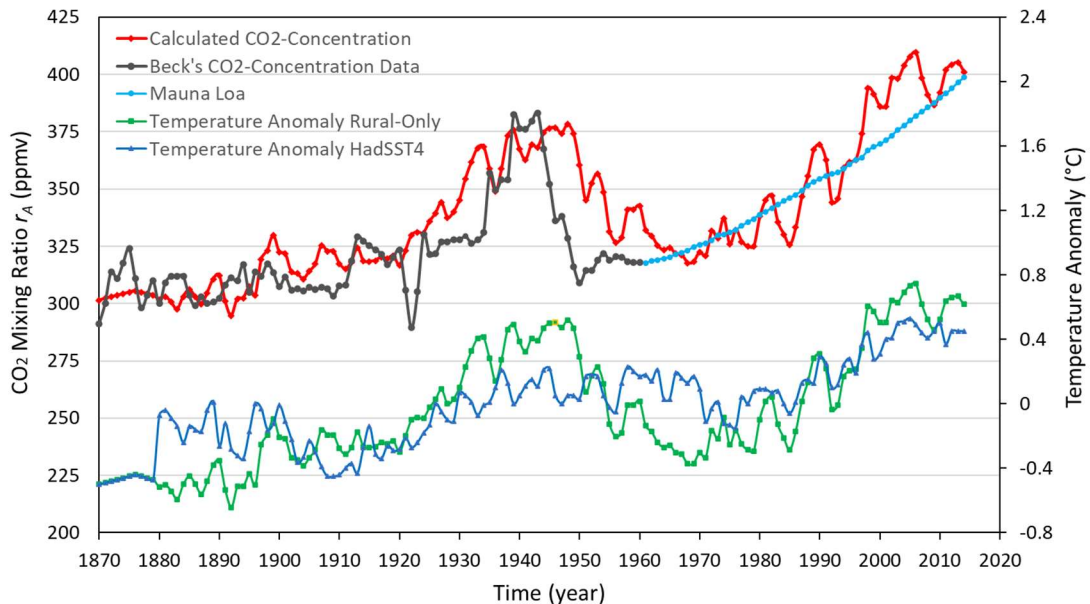


Fig. 2: Comparison of Beck's historical CO<sub>2</sub> data (Dark Dots) with calculation (Red Diamonds) for  $Q_L = 30\%/^{\circ}\text{C}$  and  $Q_O = 3\%/^{\circ}\text{C}$ . The land emission  $E_L$  is assumed to be twice the oceanic emission  $E_O$ . Mauna Loa observations (Light Blue Dots, CDIAC 2017), Northern Hemisphere rural land air temperature (Green Squares), global Sea Surface Anomaly HadSST4 (Blue Triangles).

### 3. Conclusion

An extensive compilation of almost 100.000 historical data about CO<sub>2</sub> concentration measurements between 1826 and 1960 has been published as post mortem memorial edition of the late Ernst-Georg Beck (Beck 2022). Different to the widely used interpretation of proxy data, Beck's compilation contains direct measurements of chemically analysed air samples with much higher accuracy and time resolution than available from ice core or tree ring data.

At the same time this compilation covers a period, which is of fundamental importance to understand climatic processes from the Little Ice Age up to the implementation of infrared spectroscopy

analyses in 1958. Particularly shorter variations over the 19<sup>th</sup> and 20<sup>th</sup> century and a documented significant increase of the atmospheric CO<sub>2</sub> concentration around 1940 allows to study how far, above all, natural processes have to be made responsible for these perturbations.

In this contribution we compare the temperature sensitivity of oceanic and land emissions and their expected contributions to the atmospheric CO<sub>2</sub> mixing ratio. Our simulations with a land-air temperature series (Soon et al. 2015) alone, or in combination with sea surface data (HadSST4, Kennedy et al. 2019) can well reproduce the increased mixing ratio over the 30s to 40s, the consecutive decline over the 50s and the additional rise up to 2010. This stronger variation cannot be explained only by fossil fuel emissions, which show a monotonic increase over the Industrial Era.

Particularly soil respiration in the tropics and mid-latitudes can be identified as the main natural source of CO<sub>2</sub> emissions. Smaller deviations in the maximum and width between observation and calculation of the mixing ratio around 1940 may be explained by some local impacts of the historic CO<sub>2</sub> concentration data (mostly covering the coast of the North Sea, Barents Sea and Northern Atlantic), they may also result from a smaller mismatch between the main emission areas and the covered temperature data (Northern Hemisphere), and also the time constants, before quasi equilibrium can be established in temperature and concentration, can cause some deviations. For direct comparison of the data, we avoided averaging over longer periods.

But most important, our studies not only show a high correlation of observation and calculation, but also give a clear physical explanation with a quantitative reproduction of the observed data, based on independent measurements of the temperature sensitivity of oceanic and land emission.

Anyone who has doubts about the historical CO<sub>2</sub>-data and relies on indirect proxy data, must also have doubts about the temperature trends, not only over the 30s to 50s, but up to the present.

## Funding

This work did not receive any funding.

**Guest-Editor:** Prof. Jan-Erik Solheim; Reviewers are anonymous.

## Acknowledgements

We express our special thanks to Prof. H. Yndestad and Prof. J.-E Solheim for having made available the historical CO<sub>2</sub> data of the late Ernst-Georg Beck to a broader readership. We also thank the reviewers for some additional incitements.

## References

- Beck, E.-G., 2022: *Reconstruction of Atmospheric CO<sub>2</sub> Background Levels since 1826 from Direct Measurements near Ground*, Science of Climate Change, Vol 2.2, pp. 148-211, <https://doi.org/10.53234/scc202112/16>.
- Brechet, L., Lopez-Sangil, L., George, C., Birkett, A., Baxendale, C., Trujillo, B., and E. Sayer, 2018: *Distinct responses of soil respiration to experimental litter manipulation in temperature woodland and tropical forest*, Ecol and Evolution, Vol. 8, pp. 3787-3796.
- CDIAC, 2017: Carbon Dioxide Information Analysis Center, [http://cdiac.ornl.gov/trends/emis/glo\\_2014.html](http://cdiac.ornl.gov/trends/emis/glo_2014.html).
- Engelbeen, F., 2023: *About historical CO<sub>2</sub> levels - Discussion of Direct Measurements near Ground since 1826 by E.-G. Beck*, Science of Climate Change, Vol. 3.2, pp. 190-208 <https://doi.org/10.53234/SCC202301/33>.

Feely, R., Sabine, C., Takahashi, T., and R. Wanninkhof, 2001: *Uptake and storage of carbon dioxide in the ocean: The global CO<sub>2</sub> survey*, *Oceanography*, 14, 18-32.

Harde, H., 2017: *Scrutinizing the carbon cycle and CO<sub>2</sub> residence time in the atmosphere*, *Global & Planetary Change*, 152, pp. 19-26, <http://dx.doi.org/10.1016/j.gloplacha.2017.02.009>.

Harde, H. and M. Salby, 2021: *What controls the atmospheric CO<sub>2</sub> level?* *Science of Climate Change*, Vol.1, No.1, pp. 54 - 69, <https://doi.org/10.53234/scc202106/22>

IPCC Fifth Assessment Report (AR5), 2013: T. F. Stocker, D. Qin, G.-K. Plattner, M. Tignor, S. K. Allen, J. Boschung, A. Nauels, Y. Xia, V. Bex, P. M. Midgley (Eds.): *Climate Change 2013: The Physical Science Basis. Contribution of Working Group I to the Fifth Assessment Report of the Intergovernmental Panel on Climate Change*, Cambridge University Press, Cambridge, United Kingdom and New York, NY, USA.

IPCC Sixth Assessment Report (AR6), 2021: V. Masson-Delmotte, P. Zhai, A. Pirani et al.: *Climate Change 2021: The Physical Science Basis. Contribution of Working Group I to the Sixth Assessment Report of the Intergovernmental Panel on Climate Change*, Cambridge University Press.

Kennedy, J. J., N. A. Rayner, C. P. Atkinson and R. E. Killick, 2019: *An Ensemble Data Set of Sea Surface Temperature Change From 1850: The Met Office Hadley Centre HadSST.4.0.0.0 Data Set*, *Journal of Geophysical Research: Atmospheres* 124, pp. 7719–63.

Lloyd, J. and J. Taylor, 1994: *On the temperature dependence of soil respiration*, *Functional Ecology*, 8 315-323.

Maier, M., Gartiser, V., Schengel, A., and V. Lang, 2020: *Long term gas monitoring as tool to understand soil processes*, *Appl. Sci.*, 10, 8653-8683.

Nottingham, A., Baath, E., Reischke, S., Salinas, N., and P. Meir, 2018: *Adaptation of soil microbial growth to temperature: Using a tropical elevation gradient to predict future changes*, *Glob. Change Biol.*, 25, 827-838.

Palmer, P., L. Eng, D. Baker, F. Chevallier, H. Bosch and P. Somkuti, 2019: *Net carbon emissions from African biosphere dominate pan-tropical atmospheric CO<sub>2</sub> signal*, *Nature Comm.*, <https://doi.org/10.1038/s41467-019-11097-w>.

Raich, J. W., W. H. Schlesinger. 1992. *The global carbon dioxide flux in soil respiration and its relationship to vegetation and climate*, *Tellus* 44 B, pp. 81-99.

Salby, M., H. Harde, 2022: *Theory of Increasing Greenhouse Gases*, *Science of Climate Change*, Vol 2.3, pp. 212-238, <https://doi.org/10.53234/scc202212/17>.

Soon, W., R. Connolly, and M. Connolly, 2015: *Re-evaluating the role of solar variability on Northern Hemisphere temperature trends since the 19th century*, *Earth-Science Reviews*, vol. 150, pp. 409–452.

Takahashi, T., Feely, R., Weiss, R., Wanninkhof, R., Chipman, D., Sutherland, S. and T. Takahashi, 1997: *Global air-sea flux of CO<sub>2</sub>: An estimate based on measurements of sea-air pCO<sub>2</sub> difference*, *Proc. Nat. Acad. Sci. USA*, 94, 8292-8299.

Wanninkhof, R., 2014: *Relationship between wind speed and gas exchange over the ocean revisited*. *Limnol Oceanogr. Methods*, 12, 351-362.

Wood, T., Detto, M., and W. Silver, 2013: *Sensitivity of soil respiration to variability in soil moisture and temperature in a humid tropical forest*, *PLOS ONE*, 8, <https://doi.org/10.1371/journal.pone.0080965>.

Yndestad, H., 2022: *Publication of Ernst-Georg Beck's Atmospheric CO<sub>2</sub> Time Series from 1826-1960*, *Science of Climate Change*, Vol. 2.2, pp. 134-136, <https://doi.org/10.53234/scc202112/15>.

Zhou, Z., Jian, L., Du, E., Hu, H., Li, Y., Chen, D., and J. Fang, 2013: *Temperature and substrate*



*availability regulate soil respiration in the tropical mountain rainforests, Hainan Island, China,*  
J. Plant Ecology., Vol. 6, pp. 325-334, <https://doi.org/10.1093/jpe/rtt034>.